



CrossMark
 click for updates

Cite this: *RSC Adv.*, 2014, 4, 48299

Immobilization of palladium catalyst on magnetically separable polyurea nanosupport†

Suzana Natour and Raed Abu-Reziq*

This work describes a method for preparing magnetic polyurea nanoparticles (PU NPs) and their utilization as a catalyst support. The method is based on entrapment of hydrophilic magnetic nanoparticles within the polyurea matrix. The synthetic process of these magnetic polyurea nanoparticles is based on oil-in-oil nanoemulsification of an organic polar phase comprised of *N,N*-dimethylacetamide (DMAc), 2,6-diaminopyridine and ionic liquid modified magnetite nanoparticles (MNPs-IL), in heptane containing a suitable surfactant. This was followed by interfacial polycondensation reaction between an isocyanate monomer, polymethylenepolyphenyl isocyanate (PAPI 27), and the amine monomer producing magnetically separable polyurea nanoparticles. Subsequently, these particles were employed as a catalyst nanosupport. Two catalytic systems based on the encapsulation of Pd(OAc)₂ within magnetic PU NPs or their adsorption on the surface of these particles were produced and subjected to hydrogenation reactions and selective hydrogenations of α,β -unsaturated compounds. Pd(OAc)₂ adsorbed on the surface of the magnetic PU NPs demonstrated high catalytic activity and selectivity, which was superior to the conventional catalyst Pd/C or palladium nanoparticles supported directly on the surface of magnetite nanoparticles. The catalyst was easily recovered from the reaction mixture by applying an external magnetic field and recycled over five times without observing any significant loss in its catalytic efficiency.

Received 18th August 2014
 Accepted 24th September 2014

DOI: 10.1039/c4ra08864f

www.rsc.org/advances

Introduction

Heterogeneous catalysts are designed to enable their isolation and recovery from the reaction media, while maintaining catalytic efficiency. General approaches for heterogenization of catalysts include microencapsulation within polymeric capsules,¹ and immobilization on solid surfaces such as silica particles,² organic polymer supports such as polystyrene³ and organic-inorganic hybrid mesoporous supports.⁴ However, conventional heterogeneous catalysts are significantly less active compared to their homogeneous counterparts. This led to the development of new systems, combining the merits of both catalytic approaches, called nanocatalysts or nanoreactors.⁵ Nevertheless, these systems are difficult to isolate and recover from the reaction media, sometimes requiring expensive and time consuming procedures. Therefore, a new approach based on magnetic isolation has been developed.⁶

Magnetic nanoparticles (MNPs) with their large surface area to volume ratio are subjected to extensive investigation and application in various disciplines including, catalysis,⁷ drug delivery,⁸ magnetic resonance imaging,⁹ magneto-thermal therapy¹⁰ and biomolecular sensors.¹¹ Recently, super-paramagnetic Fe₃O₄ nanoparticles were used as highly efficient catalyst supports because they provide easy accessibility to the catalytic sites and facile isolation from the reaction media by applying an external magnetic field.¹² Nonetheless, the MNPs tend to agglomerate within a short period of time. To overcome such difficulties, the surface of the Fe₃O₄ nanoparticles was modified using various methods such as a surface capping method using small capping agents like oleic acid¹³ and silane reagents.¹⁴ Likewise, a surface coating method with organic polymer shells such as polyvinyl pyrrolidone (PVP),¹⁵ polyaniline (PANI)¹⁶ and polyglycidyl methacrylate (PGMA)¹⁷ or an inorganic shell such as silica produced through the sol-gel method.^{12d,18} In the development of this field, a great emphasis has been paid towards the immobilization of numerous catalysts on the surface of Fe₃O₄ and their applications in catalysis. Among recent achievements are immobilization of metal nanoparticles, palladium based catalysts and rhodium catalyst on the surface of MNPs.^{15a,19} These catalysts proved to be highly efficient in a wide range of catalytic transformations including hydroformylation, hydrogenation, and other C-C coupling reactions.^{6b,7} This concept not only simplifies the work-up

Institute of Chemistry, Casali Center of Applied Chemistry and Center for Nanoscience and Nanotechnology, The Hebrew University of Jerusalem, Jerusalem 91904, Israel. E-mail: Raed.Abu-Reziq@mail.huji.ac.il; Fax: +972-2-6585469

† Electronic supplementary information (ESI) available: SEM and TEM images, Size distribution, EDX graph, IR spectrum and XRD pattern of MNPs, MNP-IL-C₄, PU NPs and magnetic PU NPs. XPS spectra of Pd_{ad} and Pd_{en} systems before and after hydrogenation reactions. Catalytic results of hydrogenation reactions catalysed by Pd_{ad} and Pd_{en} systems. See DOI: 10.1039/c4ra08864f

procedure but also minimizes the use of additional organic solvents and chemicals during the separation process.

Polyurea nanoparticles and nanocapsules have been mainly utilized for pharmaceutical and biomedical applications due to their stability and biocompatibility.²⁰ Conversely, magnetite nano-particles were encapsulated or entrapped mostly in silica SiO₂ nanospheres,²¹ polystyrene,²² polymethacrylate/poly-hydroxymethacrylate,²³ poly (urea-formaldehyde)²⁴ and poly-acrylamide.²⁵ The current demands toward the production of robust, expeditious and efficient catalyst supports, being rapidly and easily separated, have motivated us into developing new magnetically separable polyurea nanoparticles, in which the features of both polyurea and magnetic nanoparticles are fused. Polyurea systems have added an advantage over other catalyst supports due to its facile and relatively prompt synthetic process. The immobilization of catalytic species such as metal nanoparticles could be achieved either by encapsulation or adsorption on the surface of the magnetic polyurea nanocomposites.

Recently, we have reported a new nanoreactor based on encapsulation of palladium nanoparticles stabilized by hyper-branched polyamidoamine modified with palmitoyl groups along with hydrophobic magnetite nanoparticles within polyurea core-shell nanocapsules. The nanocapsules were synthesized by nanoemulsification of oil in water followed by interfacial polymerization between amine and isocyanate monomers. This catalytic nanoreactor exhibited catalytic activity in hydrogenation reactions in aqueous medium.²⁶ Our continuing interest in developing efficient catalyst supports led us to investigate the efficiency of magnetic polyurea nanoparticles as a catalyst support. To the best of our knowledge, entrapment of MNPs within polyurea nanoparticles with solid core, synthesized from oil in oil nanoemulsions, has not been reported yet.

Herein, we developed a new magnetically separable polyurea NPs containing coordinative groups in the shell that can conjugate and support the catalytic species. Synthesis, characterization and catalytic applications of supported palladium acetate, Pd(OAc)₂ on biocompatible and nitrogen containing magnetic polyurea nanoparticles is described. The structure of this nano-system is composed of a solid core containing hydrophilic magnetite nanoparticles and a polyurea matrix. This system has been prepared by nano-emulsification of an oil phase containing the MNPs and 2,6-diaminopyridine with another oil phase including a proper surfactant, followed by addition of polymethylene polyphenyl isocyanate (PAPI 27) to initiate an interfacial poly-condensation reaction and to create the polyurea matrix. Subsequently, Pd(OAc)₂ entrapped within or adsorbed on the surface of these magnetic polyurea nanoparticles, is utilized in hydrogenation reactions and selective hydrogenations of α,β -unsaturated compounds. The catalytic system based on adsorption of Pd(OAc)₂ exhibited in both transformations high catalytic activity and recyclability over five times without any significant loss in its catalytic efficiency.

Results and discussion

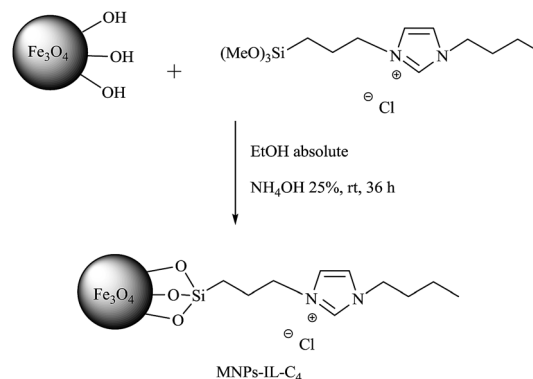
Preparation of magnetite nanoparticles modified by ionic liquid

MNPs were synthesized by employing various techniques such as, thermal decomposition,²⁷ high pressure hydrothermal methods,²⁸ a microemulsion route²⁹ or co-precipitation from aqueous solutions.^{12c} In this study, MNPs were synthesised *via* co-precipitation of iron salts, FeCl₂ and FeCl₃ in a basic aqueous solution under inert conditions at 85–90 °C according to Massart's method.³⁰ In agreement with previous reports,^{13c,30,31} MNPs formed *via* the aforementioned route were spherical in shape and small in diameter (5–20 nm) as confirmed by transmission electron microscopy (TEM) analysis (ESI, Fig. S1a†). However, particles in this size range are intrinsically unstable and tend to agglomerate in order to reduce the energy associated with the high surface area to volume ratio. In addition, non-modified MNPs are scarcely soluble in any medium. In order to surpass these restrictions, various surface modification and protection strategies of the bare MNPs have been introduced.^{12c,18a} We have covalently grafted the ionic liquid 1-butyl-3-(3-(trimethoxysilyl) propyl)-1*H*-imidazol-3-olide (IL-C₄) on the surface of magnetite NPs in order to stabilize and to enhance their solubility in a wide range of organic and aqueous solvents. The ionic liquid IL-C₄ was synthesized by reacting 3-chloropropyltrimethoxysilane with 1-butyl imidazole at 120 °C in solvent free and inert atmosphere conditions.

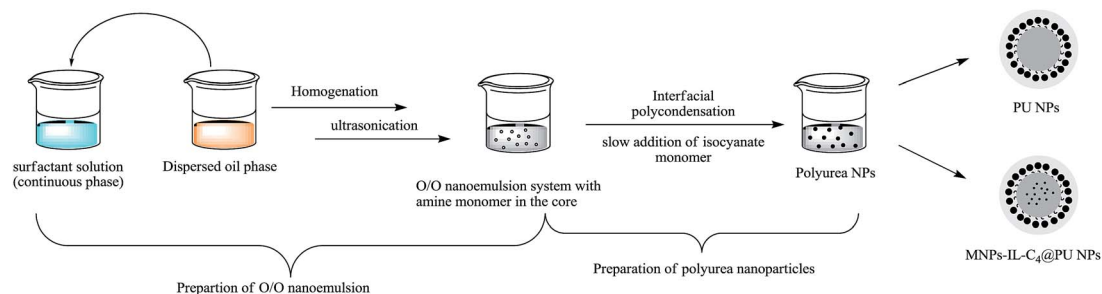
Grafting the IL-C₄ on the surface of the MNPs was carried out by reacting the trimethoxysilane groups of the IL-C₄ with the surface hydroxyl groups of the MNPs in ethanol for 36 h at room temperature (Scheme 1). The resulting MNPs-IL-C₄ shows no significant increase in the particle size, as depicted in TEM (ESI, Fig. S1b†). The loading of IL-C₄, as determined by thermogravimetric analysis (TGA), was 0.32 mmol g⁻¹. Moreover, those modified particles were highly soluble in polar organic solvents like dimethyl sulfoxide (DMSO), dimethylformamide (DMF), methanol, *N,N*-dimethyl acetamide (DMAc) and water.

Synthesis and characterization of PU NPs and magnetic polyurea nanoparticles (MNPs@PU NPs)

An optimal composition for preparing PU NPs has been established. This system has been accomplished from an oil-in-oil (O/O)



Scheme 1 Modification of magnetic NPs with IL-C₄.



Scheme 2 Illustration of preparation of polyurea nanoparticles.

nanoemulsion *via* an interfacial polycondensation process of the isocyanate monomer, PAPI 27, and diamine monomer, 2,6-diaminopyridine, with a molar ratio of 1 : 1. The synthetic route of PU NPs is depicted in Scheme 2. Concisely, fabrication of the nanoparticles from the nanoemulsion system was initiated by emulsifying the dispersed oil phase, the surfactant solution composed of heptane and the lipophilic polymeric surfactant poly(1-ethenyl pyrrolidin-2-one/hexadec-1-ene) (Agrimer AL 22), followed by ultrasonication for 10 minutes. Subsequently, PAPI 27 dissolved in xylene was slowly added while sonicating the nanoemulsion system for 3 minutes. The interfacial polycondensation reaction occurred through the nucleophilic attack of amine groups on the carbonyl groups of the isocyanate monomer. After establishing the ideal PU NPs composition, it was utilized for the incorporation of the MNPs-IL-C₄ into the cores of PU NPs by dissolving 0.4 wt% MNPs-IL-C₄ in the dispersed oil phase following the same procedure. The surface morphology and size distribution of the NPs were examined by scanning electron microscope (SEM) analysis, which revealed the formation of spherical particles with a smooth surface in both pure PU NPs (Fig. 1a) and MNPs-IL-C₄@PU NPs systems (Fig. 1b). Dynamic light scattering (DLS) studies revealed polydispersed systems with an average particles size of 230 nm and 450 nm in both PU NPs and magnetic PU NPs systems respectively (ESI, Fig. S2[†]). These results are in good agreement with the SEM results.

Furthermore, the characterization of the PU NPs and the magnetic PU NPs were carried out by TEM as illustrated in Fig. 2. The TEM micrographs confirmed the formation of polydispersed PU NPs (Fig. 2a) in addition to the successful incorporation of the MNPs within the core of PU NPs (Fig. 2b).

The complete polymerization of the amine with the isocyanate monomers was confirmed *via* infrared (IR) analysis (ESI, Fig. S3[†]). The presence of absorbance peaks at 3360 cm⁻¹ and 1690 cm⁻¹ which are assigned to the N-H and C=O stretching vibration respectively, indicate the formation of polyurea. Additionally, the absence of the absorbance peak of the isocyanate group (-C=N=O) at 2260 cm⁻¹ indicates the complete consumption of the isocyanate monomer.

Thermogravimetric analysis (TGA) of the pure MNPs, MNPs-IL-C₄, pure PU NPs and MNPs-IL-C₄@PU NPs are shown in Fig. 3. The thermal decomposition analyses were carried out in the temperature range of 25–950 °C under air. It has been noticed that there is an increase in the organic content in the modified MNPs-IL-C₄ (Fig. 3b), with 7.3% weight loss compared to the bare MNPs (Fig. 3a) with weight loss of 3.5% which could be due to absorbed moisture and solvent residues. Furthermore, the pure PU NPs showed 100% weight loss, which is concord to the fact that only organic content is present (Fig. 3d), whereas the magnetic PU NPs contained 87% organic content (Fig. 3c). Both PU NPs systems experienced several steps of degradation. In the PU NPs system (Fig. 3d), the initial weight loss is observed from 25–125 °C probably due to the presence of solvents such as heptane. The weight loss at temperatures higher than 300 °C is contributed to the decompositions of the polyurea shell and the surfactant Agrimer AL 22. Thermal decomposition of the MNPs-IL-C₄@PU NPs system (Fig. 3c) exhibits analogous behaviour to the pure PU NPs. However, the presence of the magnetic nanoparticles can accelerate the decomposition of the organic materials especially when the analysis is performed under air.

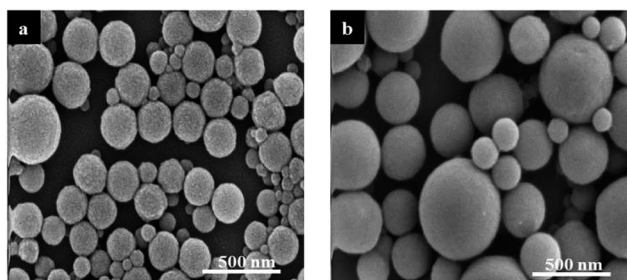


Fig. 1 SEM micrographs of (a) pure PU NPs and (b) MNPs-IL-C₄@PU NPs.

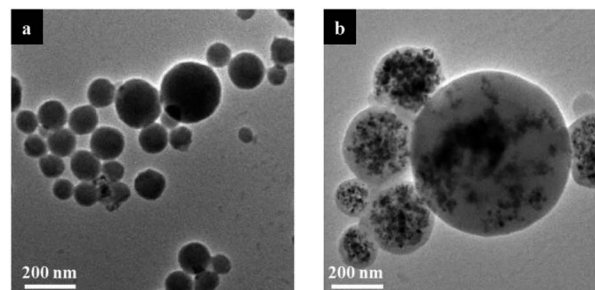


Fig. 2 TEM micrographs of (a) pure PU NPs and (b) MNPs-IL-C₄@PU NPs.

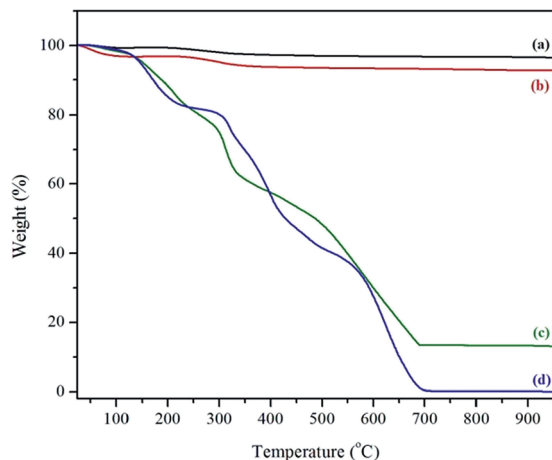


Fig. 3 TGA analysis for (a) bare MNPs; (b) MNPs-IL-C₄; (c) MNPs-IL-C₄@PU NPs and (d) pure PU NPs.

Immobilization of palladium acetate Pd(OAc)₂

Palladium is arguably the most widely used transition metal in catalysis.³² Since noble metals are extremely precious, several strategies for the heterogenization of homogeneous catalysts and metal NPs have been developed. For example, Bradley and coworkers reported an active and recyclable cross-linked resin captured palladium catalyst which was utilized in Suzuki cross-coupling reactions.³³ Microencapsulation of palladium species within polyurea microcapsules were reported by DeAlmeida *et al.*³⁴ and Zhou *et al.*³⁵ and were proven, respectively, to be effective and recyclable for Suzuki coupling reactions and reductive ring-opening hydrogenolysis of epoxides. In these studies, the catalysts were recovered from the reaction mixture by either filtration or centrifugation techniques. In our study, magnetic polyurea NPs were designed and utilized as a catalyst support in which the catalysts could be either entrapped in the core or adsorbed on the surface.

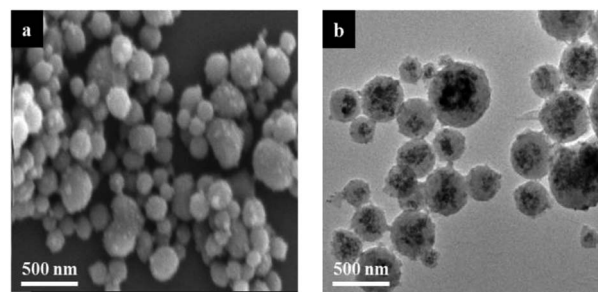


Fig. 4 Micrographs of Pd_{ad} on the surface of MNPs-IL-C₄@PU NPs determined by (a) SEM and (b) TEM.

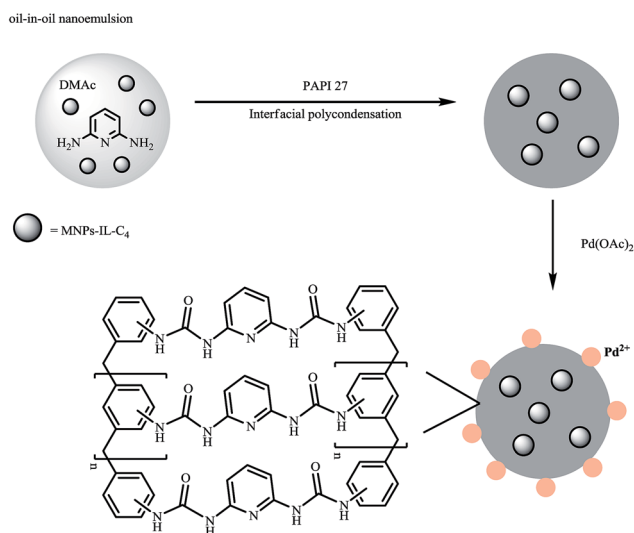
Adsorption of Pd(OAc)₂ on MNPs-IL-C₄@PU NPs

After establishing a method for the production of MNPs-IL-C₄@PU NPs, their efficiency as catalyst support was examined. Hence, Pd(OAc)₂ was physically adsorbed on the surface of the magnetic PU NPs (Pd_{ad}) by mechanically stirring the MNPs-IL-C₄@PU NPs with palladium acetate in 80 mL THF for 24 h. The resulted suspension was magnetically separated, washed twice with heptane and redispersed in heptane to reach a 20 g suspension total. This process is illustrated in Scheme 3. The loading of the adsorbed palladium according to inductively coupled plasma mass spectrometry measurements (ICP-MS) was 0.09 mmol g⁻¹. To ascertain the presence of the palladium on the surface of the magnetic PU NPs, morphology and size distribution, SEM, TEM and energy-dispersive X-ray (EDS) analysis were carried out. SEM and TEM micrographs depicted in Fig. 4a and b respectively, revealed that the surface of the MNPs-IL-C₄@PU NPs became coarse. Additionally, no changes in the size distribution and no leaching of MNPs-IL-C₄ from the core occurred. Scanning transmission electron microscope/energy dispersive X-ray spectroscopy (STEM/EDS) analysis indicated the presence of palladium on the surface (ESI, Fig. S4†).

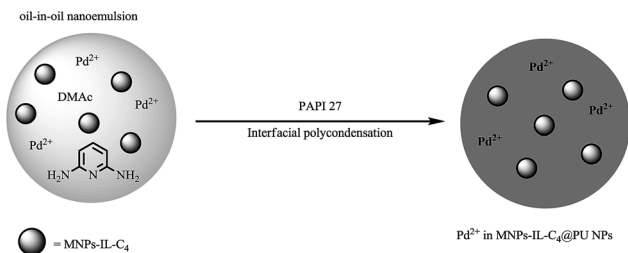
Pure magnetite NPs and Pd_{ad}/MNPs-IL-C₄@PU NPs were also analyzed by X-ray powder diffraction (XRD). The XRD pattern of the pure magnetite NPs displayed the characteristic peaks at $2\theta = 18.3, 30.1, 35.5, 43.3, 53.5, 57.1, 62.6, 71$ and 74 with cubic unit cell (ESI, Fig. S5a†). Likewise, the XRD pattern of the Pd_{ad} on MNPs-IL-C₄@PU NPs revealed identical characteristic peaks with five additional peaks at $2\theta = 40, 46.6, 67.5, 81.3$ and 85.4 which match the characteristic peaks of fcc palladium crystal structure well. These peaks are attributed to (100), (200), (220), (311) and (222) reflections respectively (ESI, Fig. S5b†).

Entrapment of Pd(OAc)₂ within the MNPs-IL-C₄@PU NPs

Second approach for immobilization of catalysts is based on incorporation of catalytic species within the core of the solid support. In this context, palladium acetate entrapped within the magnetic PU NPs (Pd_{en}) has been established. This was achieved by following the same procedure applied for the incorporation of MNPs. The palladium acetate was dissolved in the DMAc along with the MNPs-IL-C₄ and nanoemulsified in heptane. This was followed with interfacial polycondensation to



Scheme 3 Preparation of Pd_{ad} on MNPs-IL-C₄@PU NPs.



Scheme 4 Preparation of palladium incorporated within magnetic PU NPs.

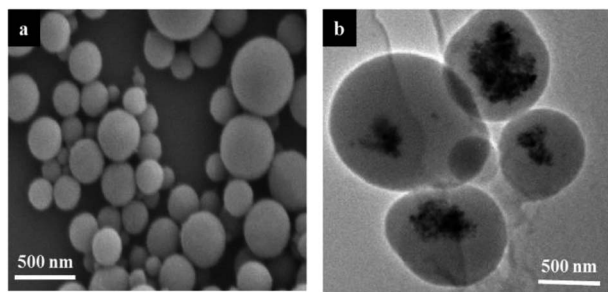


Fig. 5 Micrographs of entrapped $\text{Pd}(\text{OAc})_2$ within MNPs-IL- C_4 @PU NPs determined by (a) SEM and (b) TEM.

produce polyurea NPs. Preparation route is illustrated in Scheme 4. The resulted suspension was magnetically separated, washed with heptane and redispersed in heptane to reach a 20 g suspension total. SEM and TEM micrographs of Pd_{en} system are depicted in Fig. 5. The STEM/EDS analysis (ESI, Fig. S6[†]) indicated the presence of palladium in the PU NPs matrix.

Supporting palladium on the surface of MNPs-IL- C_4

Heterogenization of metal NPs can be further achieved by means of a deposition and immobilization directly onto the surface of solid supports and functionalized MNPs. Herein, in order to confirm that polyurea matrix is indeed essential for supporting metal nanoparticles and for obtaining high catalytic activity and selectivity, we further investigated the capability of the MNPs-IL- C_4 to operate as a catalyst support. In this regard, the Pd NPs were directly immobilized on the surface of the modified ionic liquid MNPs simply by exposing the MNPs-IL- C_4 dispersed in ethanol to a solution of Na_2PdCl_4 followed by reduction with either NaBH_4 or hydrazine hydrate affording supported Pd NPs (Scheme 5).

The supported palladium NPs system was analyzed by TEM (ESI, Fig. S7a[†]). The palladium NPs were not easily recognized in the TEM analysis when they were immobilized directly on the

surface of the MNPs-IL- C_4 . Hence, EDS analysis was carried out and it confirmed the presence of the palladium on the MNPs-IL- C_4 (ESI, Fig. S7b[†]).

Catalysis

Hydrogenation reaction was utilized as a model reaction in order to probe the catalytic efficiency of both Pd_{ad} and Pd_{en} catalytic systems.

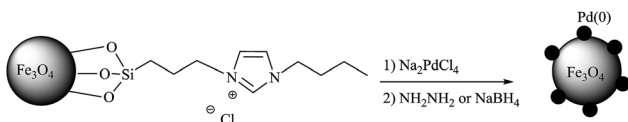
The catalytic performance of Pd_{ad} was initially tested with various substrates under reaction conditions of stirring at 50 °C for 2 h with a total pressure of 40 psi of hydrogen. The results are summarized in ESI, Table S1.[†] The catalyst exhibited high catalytic activity for the hydrogenation of styrene and its derivatives (ESI, Table S1,[†] entries 1–6) by fully converting them into the desired products. X-ray photoelectron spectroscopy (XPS) was utilized to characterize and confirm the oxidation state of the palladium before and after the hydrogenation reactions. The binding energy of Pd_{ad} system before a hydrogenation reaction of styrene exhibits two strong characteristic peaks centered at 338.2 eV and 343.4 eV, which are attributed to Pd 3d_{5/2} and Pd 3d_{3/2} respectively (ESI, Fig. S8a[†]). In addition, the binding energy peaks at 335.6 eV and 340.86 eV corresponds to the reduction of Pd(II) to Pd(0) during the reaction (ESI, Fig. S8b[†]).³⁶

In order to obtain insight as to the catalytic efficiency of the entrapped palladium within magnetically retrievable PU NPs (Pd_{en}) the same hydrogenation reactions were carried out under equal reaction conditions. The outcome displayed in ESI, Table S2[†] clearly indicates that the palladium inside the PU NPs is less active compared to that adsorbed. Even though reaction time was prolonged to 6 h, only styrene (ESI, Table S2,[†] entry 1) fully reacted. However, this cannot be said for the other substrates in which no significant change in the yield was detected (ESI, Table S2,[†] entries 2–4). This decrease in the reactivity of Pd_{en} system might be attributed to inaccessibility of the substrates to the catalytic sites. Furthermore, XPS analysis depicts the presence of mainly Pd(II) cations before and after catalytic hydrogenation (ESI, Fig. S9[†]). It is known that Pd(II) is less reactive than Pd(0) in hydrogenation of olefins.³⁷

Since Pd_{ad} system exhibited excellent activity compared to the Pd_{en} system, it was further investigated in the hydrogenation of various unsaturated organic compounds. Table 1 displays high activity of Pd_{ad} in the hydrogenation of vinyl arenes (Table 1, entry 1) and simple aliphatic alkenes (Table 1, entries 2–7), in addition to aromatic alkynes (Table 1, entries 8–11), in which full conversions were achieved. Simultaneously, and under identical reaction conditions, hydrogenation of 3-methylstyrene was carried out using commercial Pd/C (10%) yielding 64% of the desired product (Table 1, entry 12).

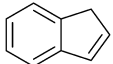
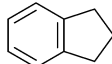
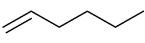
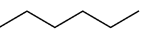
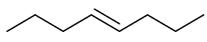
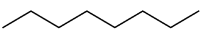
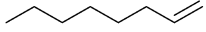
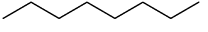
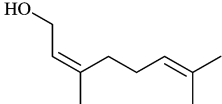
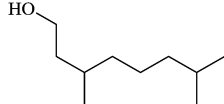
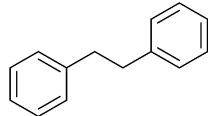
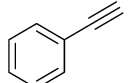
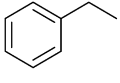
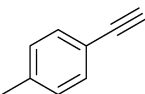
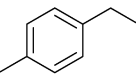
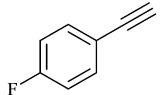
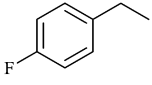
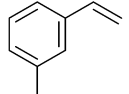
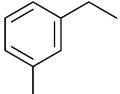
Selective hydrogenation reaction of α,β -unsaturated compounds

Selective, and particularly chemoselective, catalytic hydrogenation of α,β -unsaturated organic compounds is an essential and desirable process in synthetic chemistry and chemical industries.³⁸ The hydrogenation of C=C and C=O bonds is



Scheme 5 Palladium NPs supported on MNPs-IL- C_4 .

Table 1 Hydrogenation of alkenes and alkynes by Pd_{ad}/MNPs-IL-C₄@PU NPs^a

Entry	Substrate	Product ^b	Yield ^c (%)
1			94
2			100
3			100
4			100
5			100
6			100
7			96
8			100
9			100
10			100
11			100
12 ^d			64

^a Reaction conditions: 1.1 g of the Pd_{ad}/MNPs-IL-C₄@PU NPs suspension in heptane containing 0.008 mmol of palladium catalyst, 1.6 mmol substrate in 5 mL heptane, 40 psi hydrogen, 2 h at 50 °C.

^b Characterized by ¹H-NMR spectroscopy. ^c Determined by ¹H-NMR spectroscopy and GC. ^d Reaction conditions: 0.5 mol% Pd/C (10%), 40 psi hydrogen, 2 h at 50 °C and 6 mL heptane.

thermodynamically viable, producing valuable saturated carbonyl and unsaturated alcohol compounds which can be utilized as intermediates for synthesizing fine chemicals, pharmaceuticals, flavoring materials and biological active compounds.³⁹ Various metal nanoparticles, amongst them palladium, have been utilized to serve this aim.⁴⁰ Traditionally, Pd based catalysts are employed for the selective hydrogenation of C=C bonds yielding saturated carbonyl compounds. Encouraged by the results obtained in the hydrogenation

reactions and with the optimized reaction conditions, the scope of the Pd_{ad} catalytic system was further examined in the selective hydrogenation of α,β -unsaturated organic compounds as displayed in Table 2. First, we attempted to examine the catalytic performance of Pd_{ad} system in the selective hydrogenation of cinnamaldehyde at room temperature (Table 2, entry 1) 17% conversion with 15% yield in favour of the saturated carbonyl compounds was obtained. When the same reaction was carried out at 50 °C for 2 h, the reaction proceeded to completion with 92% yield (Table 2, entry 2). It is noteworthy that the selective hydrogenation of unsaturated aldehydes led to the production of minor amounts of unsaturated alcohols (Table 2, entries 2–4). Whereas, the Pd_{ad} system proved to be highly efficient and extremely selective for the hydrogenation of C=C bonds while keeping the carbonyl and the nitro group intact, when unsaturated ketones (Table 2, entries 5–9), unsaturated esters (Table 2, entries 11, 12) and unsaturated nitro compound (Table 2, entry 10) were employed. In addition, the selective hydrogenation of cinnamaldehyde with the commercially available Pd/C 10% (Table 2, entry 13) was examined. 85% conversion with 67% yield of the saturated carbonyl product was obtained. In addition, when the same reaction was performed under homogeneous conditions using Pd(OAc)₂, 20% conversion was obtained with 14% yield (Table 3, entry 1).

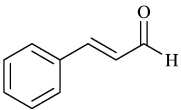
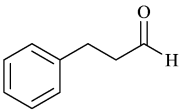
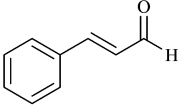
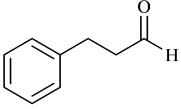
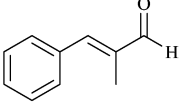
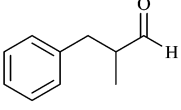
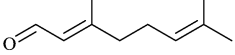
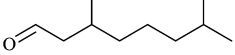
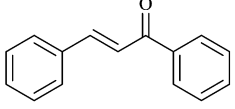
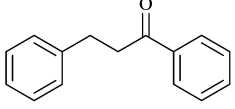
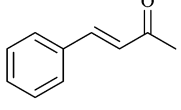
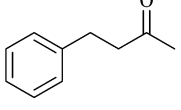
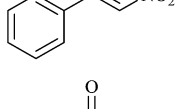
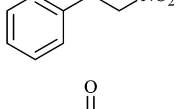
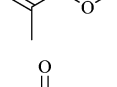
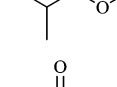
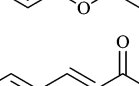
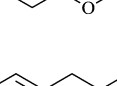
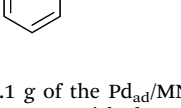
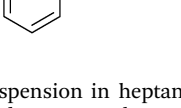
For further confirmation that our catalyst support is highly efficient and that the presence of PU matrix is indispensable for obtaining high conversions and selectivities, the Pd NPs supported on MNPs was tested in the hydrogenation of cinnamaldehyde as a control reaction. When hydrazine hydrate was used as the reducing agent only 14% conversion was obtained (Table 3, entry 2). On the other hand, when NaBH₄ was applied, 40% conversion with 29% yield was obtained (Table 3, entry 3).

In order to substantiate that the catalysis is due to the supported palladium and not by leached palladium species, hot filtration test was carried out. Selective hydrogenation of cinnamaldehyde was conducted with Pd_{ad} system and H₂ pressure of 40 psi at 50 °C. After 30 min the catalyst was magnetically separated, and the reaction was allowed to react for further 1.5 h. We have observed that no further reaction occurred after performing the hot separation process. This outcome highly indicates that there is no palladium leaching.

Recyclability of Pd_{ad} catalytic system

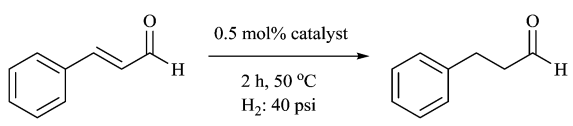
Recyclability of the heterogeneous catalysts, while preserving their catalytic efficiency, is one of the major and notable interests due to the environmental concerns. Hence, by incorporating the MNPs-IL-C₄ into the core of the PU NPs, the separation of the product and recovery of the catalyst was easily accomplished simply by applying an external magnetic field. The reusability of the catalyst was assessed in the hydrogenation of 3-methyl styrene and selective hydrogenation of 3-methylcyclohexenone, under the optimized reaction conditions. After each run the catalyst was separated and recycled by applying an external magnetic field, washed with heptane and used directly in the next cycle without further purifications. The recovered catalyst exhibited remarkable efficiency and

Table 2 Selective hydrogenations of α,β -unsaturated organic compounds catalyzed by Pd_{ad}/MNPs-IL-C₄@PU NPs^d

Entry	Substrate	Product ^b	Conversion ^c %	Yield ^d %
1 ^e			17	15
2			100	92
3			100	98
4			100	98
5			96	96
6			100	100
7			100	100
8			100	100
9			100	100
10			100	100
11			100	100
12			100	100
13 ^f			85	67

^a Reaction conditions: 1.1 g of the Pd_{ad}/MNPs-IL-C₄@PU NPs suspension in heptane containing 0.008 mmol of palladium catalyst, 1.6 mmol substrate in 5 mL heptane, 40 psi hydrogen, 2 h at 50 °C. ^b Products were characterized by ¹H-NMR spectroscopy. ^c Determined by ¹H-NMR spectroscopy and GC. ^d Determined by GC. ^e Reaction carried out at room temperature. ^f Reaction conditions: 0.5 mol% Pd/C (10%), 40 psi hydrogen, 2 h at 50 °C and 6 mL heptane.

Table 3 Selective hydrogenation of cinnamaldehyde



Entry	Catalyst	Conversion ^b (%)	Yield ^c (%)
1 ^a	Pd(OAc) ₂	20	14
2 ^d	Pd(0)/MNPs-IL-C ₄	14	12
3 ^e	Pd(0)/MNPs-IL-C ₄	40	29

^a Reaction conditions: 0.009 mmol of catalyst, 1.8 mmol cinnamaldehyde, 40 psi hydrogen, 2 h at 50 °C, 6 mL heptane and 0.3 mL CH₂Cl₂. ^b Products were characterized by ¹H-NMR spectroscopy. ^c Determined by ¹H-NMR spectroscopy and GC. ^d Reducing agent: hydrazine hydrate, Reaction conditions: 2 g of the dispersed catalyst in heptane containing 0.008 mmol palladium catalyst, 1.6 mmol cinnamaldehyde in 3 mL heptane, 50 °C, 40 psi H₂, 2 h. ^e Reducing agent: sodium borohydride. Reaction conditions: same as d but 1.6 g of dispersed catalyst in heptane containing 0.008 mmol palladium catalyst were used.

preserved its catalytic activity and selectivity while maintaining the yield at 100% even after 5 subsequent cycles.

SEM of the recycled catalytic system revealed and confirmed that the morphology and particle size distribution were not dramatically changed after three (Fig. 6a) and five cycles (Fig. 6b). In addition, TEM (Fig. 7a) and EDS (Fig. 7b) micrographs unambiguously revealed the formation and presence of Pd nanoparticles of 2–3 nm on the surface of the magnetic PU

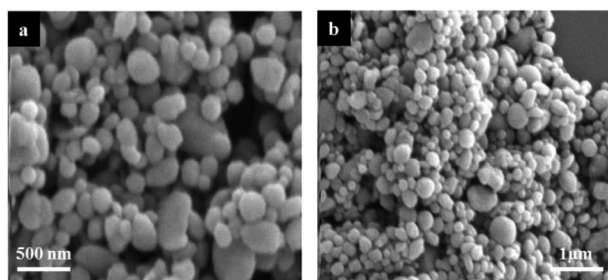


Fig. 6 SEM images of recycled catalyst after (a) 3 cycles and (b) 5 cycles.

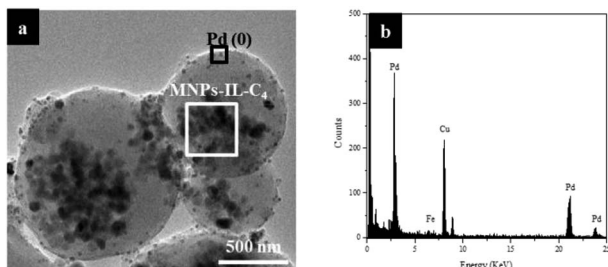


Fig. 7 (a) TEM micrograph and (b) EDS analysis of Pd NPs adsorbed on the surface of MNPs-IL-C₄@PU NPs.

NPs produced from reduction of Pd(OAc)₂ during the hydrogenation reaction. It is worth noting that no leaching of palladium was observed after the third and fifth run according to ICP-MS studies.

Conclusion

This work demonstrated the development of a new magnetically retrievable catalytic PU NPs based on adsorption of palladium acetate on the surface of the magnetic and nitrogen containing PU NPs. This new catalytic Pd_{ad} system exhibited remarkable activity and higher efficiency in hydrogenation of aromatic and aliphatic alkenes compared to the encapsulated palladium system. The scope of the catalytic Pd_{ad} system was further probed in the selective hydrogenation of aromatic and aliphatic α,β -unsaturated organic compounds demonstrating high and consistent activity and selectivity. The catalytic Pd_{ad} system, both in hydrogenation and selective hydrogenation reactions was easily isolated and reused up to 5 times without observing any significant loss in catalytic activity. In future studies, the present catalytic system will be subjected to various other catalysts and examined in other essential transformations.

Experimental section

Materials and methods

Poly(1-ethenyl pyrrolidin-2-one/hexadec-1-ene) (Agrimer AL22) and polymethylenepolyphenyl isocyanate (PAPI 27) were contributed by FMC Corporation. FeCl₃·6H₂O, FeCl₂·4H₂O, ammonium hydroxide 25% and 2,6-diaminopyridine were purchased from Acros Fischer Scientific. (3-chloropropyl) trimethoxysilane, 1-butyl imidazole, tris(2-aminoethyl)amine 96% was purchased from Sigma Aldrich. All the substrates for the hydrogenation reactions were purchased from either Sigma Aldrich or Acros and were used without further purifications. Scanning electron microscope (SEM) was utilized to determine the morphology of the PU-NPs. The experiments were performed on high resolution scanning electron microscope (HR SEM) Sirion (FEI Company) using Shottky type field emission source and secondary electron (SE) detector. The images were scanned at voltage of 5 kV. Transmission electron microscope (TEM) and electron diffraction spectroscopy (EDS) were performed with (S) TEM Tecnai F20 G2 (FEI Company, USA) operated at 200 kV. The infrared spectra were recorded at room temperature in transmission mode using a Perkin Elmer spectrometer 65 FTIR instrument. Thermogravimetric analysis (TGA) was performed on Mettler Toledo TG 50 analyzer. Measurements were carried out at temperature range that extended from 25–950 °C at a heating rate of 10 °C min⁻¹ under air. Dynamic light scattering (DLS) was utilized to determine the size distribution of the PU-NPs. These measurements were performed on Nano Series instrument of model Nano-Zeta Sizer (Malvern Instruments) model ZEN3600. Gas chromatography (GC) (Agilent Technologies, 7890A) with a capillary column (HP-5, 30 meters) was used to determine the conversion of the hydrogenation reactions. ¹H-NMR and ¹³C-NMR spectra were recorded with Bruker DRX-400 instrument in CDCl₃. Powder X-

ray diffraction (XRD) measurements were performed on the D8 Advance diffractometer (Bruker AXS, Karlsruhe, Germany) with a goniometer radius 217.5 mm secondary graphite monochromator, 2° Soller slits and 0.2 mm receiving slit. Low-background quartz sample holders were carefully filled with the powder samples. XRD patterns within the range $2\theta = 1^\circ$ to 90° were recorded at room temperature using CuK α radiation ($\lambda = 1.5418 \text{ \AA}$) with following measurement conditions: tube voltage of 40 kV, tube current of 40 mA, step-scan mode with a step size of $2\theta = 0.02^\circ$ and counting time of 1 s per step. The X-ray Photoelectron Spectroscopy (XPS) measurements were performed using a Kratos Axis Ultra X-ray photoelectron spectrometer (Kratos Analytical, Manchester, UK) using an Al K α monochromatic radiation source (1486.7 eV), pass energy 20 eV, step size 0.1 eV. The binding energies were calibrated using the C 1s energy as 285.0 eV.

Synthesis of 1-butyl-3-(3-(trimethoxysilyl)propyl)-1H-imidazol-3-ylchloride (IL-C₄)³¹

3-Chloropropyltrimethoxysilane (14.2 g, 114.3 mmol) and 1-butylimidazole (22.73 g, 114.3 mmol) were stirred under inert atmosphere at 120 °C for 24 h. The mixture was cooled down to room temperature and yellow-orange viscous liquid (35.32 g) was obtained (96% yield). ¹H NMR (400 MHz, CDCl₃) δ 0.524 (t, $J = 8 \text{ Hz}$, 3H), 0.847 (t, $J = 7.2 \text{ Hz}$, 3H), 1.25 (m, 2H), 1.81 (m, 2H), 1.91 (m, 2H), 3.45 (s, 9H), 4.27 (q, $J = 7.2 \text{ Hz}$, 4H), 7.39 (s, 1H), 7.52 (s, 1H), 10.57 (s, 1H) ppm. ¹³C NMR (100 MHz, CDCl₃) δ 5.94, 13.11, 19.27, 23.89, 32.01, 49.31, 50.12, 51.29, 121.97, 122.37, 136.48 ppm.

Preparation of magnetite nanoparticles supported IL-C₄ (MNPs-IL-C₄)

11.73 g FeCl₃·6H₂O and 4.4 g FeCl₂·4H₂O were dissolved and mechanically stirred in 400 mL deionized water under inert atmosphere. The mixture was heated at 85–90 °C followed by quick addition of 18 mL concentrated ammonia 25% generating black suspension of magnetite NPs. The mixture was heated for further 15 min, and then it was allowed to cool to room temperature. The black magnetite nanoparticles were separated *via* external magnetic force and washed 4 times with 250 mL deionized water and once with 200 mL ethanol. The magnetite nanoparticles were suspended in 400 mL ethanol and sonicated for 90 min. The suspension was mechanically stirred and a solution of 100 mL of ethanol containing 30 mmol of the functionalized IL-C₄ and 15 mL of concentrated ammonia (25%) were added and the reaction mixture was allowed to stir under nitrogen for 36 h at room temperature. The modified magnetite NPs were magnetically separated, washed three times with ethanol and once with methanol. Then MNPs were suspended in 400 mL methanol and mechanically stirred for another 3 h at room temperature. Eventually, 100 mL diethyl ether was added to the suspension and the modified magnetite NPs were magnetically separated, washed with diethyl ether and dried under vacuum for 12 h. 5 g of black magnetite NPs powder was obtained.

Preparation of polyurea nanoparticles

The polyurea nanoparticles were prepared in a typical procedure of interfacial polymerization of an oil-in-oil emulsion technique. A continuous phase composed of a surfactant solution of 5 g (5 wt %) Agrimer AL22 dissolved in 90 g of heptane was homogenized at 10 000 rpm for 30 seconds. A dispersed phase composed of a mixture of 4.65 g of *N,N*-dimethylacetamide and 2,6-diaminopyridine (0.35 g, 3.2 mmol) was then rapidly added during homogenization. The emulsification process was carried out for further 1 min and 30 seconds at 10 000 rpm followed by sonication for 10 min using ultrasonic cell disrupter with an output of 130 Watt and 20 KHz. Eventually, 1.1 g PAPI 27 dissolved in 8.9 g xylene was added slowly to the emulsion system during sonication. The mixture was then stirred for 4 h at room temperature. The resulting PU NPs were collected by centrifugation at 11 000 rpm for 15 min, washed couple of times with heptane and finally redispersed in heptane to reach a 20 g suspension total.

Preparation of magnetic PU NPs (MNPs-IL-C₄@PU NPs)

Magnetic PU NPs were prepared by incorporation of magnetite NPs-IL-C₄ into the PU NPs. 0.02 g of MNPs-IL-C₄ were dispersed in the mixture of 4.65 g *N,N*-dimethylacetamide and 2,6-diamino pyridine (0.35 g, 3.2 mmol) and sonicated in a bath sonicator for 60 min. The incorporation process has been achieved by following the same procedure and using the same amount of surfactant solution as it described in preparation of PU NPs. Lastly, the reaction mixture was mechanically stirred at room temperature for 4 h. The resulting magnetic PU NPs were separated by external magnetic field and redispersed in heptane.

Encapsulation of palladium acetate within MNPs-IL-C₄@PU NPs

Pd(OAc)₂ (36 mg, 0.16 mmol) was dissolved in the dispersed phase containing 0.02 g MNPs-IL-C₄, 4.65 g *N,N*-dimethyl acetamide and 2,6-diaminopyridine (0.35 g, 3.2 mmol) and sonicated for 60 min. Encapsulation was achieved by following the same procedure as for preparation of MNPs-IL-C₄@PU NPs. The catalytic magnetic PU NPs were separated by external magnetic field, washed three times with heptane and eventually redispersed in heptane to reach a 20 g suspension total. The loading of Pd in this system was found to be 0.1 mmol g⁻¹ according to inductively coupled plasma mass spectrometry measurements (ICP-MS).

Adsorption of Pd(OAc)₂ on the surface of the MNPs-IL-C₄@PU NPs

The prepared MNPs-IL-C₄@PU NPs were magnetically separated from heptane, washed with THF, redispersed in 80 mL THF and sonicated for 20 min. The suspension was mechanically stirred at room temperature and Pd(OAc)₂ (36 mg, 0.16 mmol) in 2 mL THF was added to the suspension and all was mixed for 24 h. The resulting catalytic system was separated *via* external magnetic field, washed twice with heptane and

redispersed heptane to reach a 20 g suspension total. The palladium loading in this system is 0.09 mmol g⁻¹ according to ICP-MS analysis.

Supporting palladium nanoparticles on ionic liquid modified magnetite nanoparticles (Pd(0)/MNPs-IL-C4)

0.5 g of the ionic liquid-modified magnetite nanoparticles were dissolved in 100 mL of ethanol and sonicated for 60 min. The suspension was mechanically stirred at room temperature and 60 mg (0.172 mmol) of Na₂PdCl₄ dissolved in 2 mL of distilled water was added. The resulted mixture was stirred for 24 h at room temperature, and then 2 mL hydrazine hydrate or 0.26 mmol sodium borohydride were added. After stirring for 6 h, the supported palladium nanoparticles were magnetically separated and washed twice with 30 mL water, twice with 20 mL ethanol and twice with 20 mL heptane. The washed nanoparticles were dissolved in 15 mL heptane. The loading of palladium was 0.12 mmol g⁻¹ when the reducing agent was hydrazine and 0.15 mmol g⁻¹ when it was sodium borohydride.

General procedure for the hydrogenation and selective hydrogenation reaction catalyzed by Pd_{ad} and Pd_{en} systems

A 25 mL glass lined autoclave was charged with 1.6 mmol substrate dissolved in 5 mL heptane and the proper amount of the catalytic system dispersed in heptane containing 0.008 mmol palladium. The autoclave was sealed, purged three times with hydrogen, and pressurized to 40 psi with hydrogen. The reaction mixture was stirred at 50 °C for 2–6 h. The autoclave was cooled to room temperature and the gas was released. The catalytic system was magnetically separated and the solution was decanted, filtered through Celite and evaporated under reduced pressure.

General procedure for the selective hydrogenation catalyzed by immobilized palladium on MNPs-IL-C₄

A 25 mL glass lined autoclave was charged with 1.6 mmol substrate dissolved in 3 mL heptane and the desired amount of Pd(0)/MNPs-IL-C₄ dispersed in heptane (containing 0.008 mmol palladium catalyst). The autoclave was sealed, purged three times with hydrogen, and pressurized to 40 psi with hydrogen. The reaction mixture was stirred at 50 °C for 2 h. The autoclave was cooled to room temperature and the gas was released. The catalytic system was magnetically separated and the solution was decanted, filtered through Celite and evaporated under reduced pressure.

Notes and references

- (a) S. Kobayashi and R. Akiyama, *Chem. Commun.*, 2003, 449–460; (b) S. L. Poe, M. Kobaslija and D. T. McQuade, *J. Am. Chem. Soc.*, 2007, **129**, 9216–9221; (c) B. P. Mason, A. R. Bogdan, A. Goswami and D. T. McQuade, *Org. Lett.*, 2007, **9**, 3449–3451.
- (a) A. Corma and H. Garcia, *Adv. Synth. Catal.*, 2006, **348**, 1391–1412; (b) T. Dohi, K.-i. Fukushima, T. Kamitanaka, K. Morimoto, N. Takenaga and Y. Kita, *Green Chem.*, 2012, **14**, 1493–1501; (c) P. Li, L. Wang, Y. Zhang and G. Wang, *Tetrahedron*, 2008, **64**, 7633–7638; (d) N. J. S. Costa and L. M. Rossi, *Nanoscale*, 2012, **4**, 5826–5834.
- T. E. Kristensen and T. Hansen, *Eur. J. Org. Chem.*, 2010, 3179–3204.
- (a) R. J. Kalbasi, M. Kolahdoozan and M. Rezaei, *J. Ind. Eng. Chem.*, 2012, **18**, 909–918; (b) S. Shylesh, Z. Zhou, Q. Meng, A. Wagener, A. Seifert, S. Ernst and W. R. Thiel, *J. Mol. Catal. A: Chem.*, 2010, **332**, 65–69.
- (a) *Nanomaterials in Catalysis*, ed. K. Philippot and P. Serp, Wiley-VCH, Weinheim, 2013; (b) D. Astruc, F. Lu and J. R. Aranzaes, *Angew. Chem., Int. Ed.*, 2005, **44**, 7852–7872; (c) S. B. Kalidindi and B. R. Jagirdar, *ChemSusChem*, 2012, **5**, 65–75; (d) V. Polshettiwar and R. S. Varma, *Green Chem.*, 2010, **12**, 743–754; (e) R. Narayanan, *Green Chem. Lett. Rev.*, 2012, **5**, 707–725; (f) B. F. G. Johnson, *Top. Catal.*, 2003, **24**, 147–159.
- (a) R. Abu-Reziq and H. Alper, *Appl. Sci.*, 2012, **2**, 260–276; (b) R. B. N. Baig and R. S. Varma, *Chem. Commun.*, 2013, **49**, 752–770.
- Y. Zhu, L. P. Stubbs, F. Ho, R. Liu, C. P. Ship, J. A. Maguire and N. S. Hosmane, *ChemCatChem*, 2010, **2**, 365–374.
- (a) T. Neuberger, B. Schoepf, H. Hofmann, M. Hofmann and R. B. Von, *J. Magn. Magn. Mater.*, 2005, **293**, 483–496; (b) A. K. Gupta and A. S. G. Curtis, *J. Mater. Sci.: Mater. Med.*, 2004, **15**, 493–496.
- Q. A. Pankhurst, J. Connolly, S. K. Jones and J. Dobson, *J. Phys. D: Appl. Phys.*, 2003, **36**, R167–R181.
- A. Jordan, R. Scholz, P. Wust, H. Fahling and R. Felix, *J. Magn. Magn. Mater.*, 1999, **201**, 413–419.
- D. L. Graham, H. A. Ferreira and P. P. Freitas, *Trends Biotechnol.*, 2004, **22**, 455–462.
- (a) C. Yang, J. Wu and Y. Hou, *Chem. Commun.*, 2011, **47**, 5130–5141; (b) T. K. Indira and P. K. Lakshmi, *Int. J. Pharm. Sci. Nanotechnol.*, 2010, **3**, 1035–1042; (c) M. Faraji, Y. Yamini and M. Rezaee, *J. Iran. Chem. Soc.*, 2010, **7**, 1–37; (d) W. Wu, Q. He and C. Jiang, *Nanoscale Res. Lett.*, 2008, **3**, 397–415; (e) A. S. Teja and P.-Y. Koh, *Prog. Cryst. Growth Charact. Mater.*, 2009, **55**, 22–45; (f) C. Hui, C. Shen, T. Yang, L. Bao, J. Tian, H. Ding, C. Li and H. J. Gao, *J. Phys. Chem. C*, 2008, **112**, 11336–11339.
- (a) T. Gong, D. Yang, J. Hu, W. Yang, C. Wang and J. Q. Lu, *Colloids Surf., A*, 2009, **339**, 232–239; (b) C. Rodriguez, M. Banobre-Lopez, Y. V. Kolen'ko, B. Rodriguez, P. Freitas and J. Rivas, *IEEE Trans. Magn.*, 2012, **48**, 3307–3310; (c) X. Liu, M. D. Kaminski, Y. Guan, H. Chen, H. Liu and A. J. Rosengart, *J. Magn. Magn. Mater.*, 2006, **306**, 248–253; (d) J. Puig, C. E. Hoppe, L. A. Fasce, C. J. Pérez, Y. Piñeiro-Redondo, M. Bañobre-López, M. A. López-Quintela, J. Rivas and R. J. J. Williams, *J. Phys. Chem. C*, 2012, **116**, 13421–13428.
- (a) H. M. R. Gardimalla, D. Mandal, P. D. Stevens, M. Yen and Y. Gao, *Chem. Commun.*, 2005, 4432–4434; (b) X. Liu, J. Xing, Y. Guan, G. Shan and H. Liu, *Colloids Surf., A*, 2004, **238**, 127–131; (c) M. Ma, Y. Zhang, W. Yu, H.-y. Shen, H.-q. Zhang and N. Gu, *Colloids Surf., A*, 2003, **212**, 219–226.

- 15 (a) R. Abu-Reziq, H. Alper, D. Wang and M. L. Post, *J. Am. Chem. Soc.*, 2006, **128**, 5279–5282; (b) Y. Hou, J. Yu and S. Gao, *J. Mater. Chem.*, 2003, **13**, 1983–1987; (c) X. Lu, M. Niu, R. Qiao and M. Gao, *J. Phys. Chem. B*, 2008, **112**, 14390–14394.
- 16 S. Xuan, Y.-X. J. Wang, J. C. Yu and K. C.-F. Leung, *Langmuir*, 2009, **25**, 11835–11843.
- 17 D. Horak and N. Benedyk, *J. Polym. Sci., Part A: Polym. Chem.*, 2004, **42**, 5827–5837.
- 18 (a) C. W. Lim and I. S. Lee, *Nano Today*, 2010, **5**, 412–434; (b) L. M. Rossi, N. J. S. Costa, F. P. Silva and R. Wojcieszak, *Green Chem.*, 2014, **16**, 2906–2933.
- 19 (a) V. Polshettiwar, R. Luque, A. Fihri, H. Zhu, M. Bouhrara and J.-M. Basset, *Chem. Rev.*, 2011, **111**, 3036–3075; (b) J. Liu, X. Peng, W. Sun, Y. Zhao and C. Xia, *Org. Lett.*, 2008, **10**, 3933–3936; (c) Z. Wang, B. Shen, A. Zou and N. He, *Chem. Eng. J.*, 2005, **113**, 27–34; (d) S. Shylesh, V. Schuenemann and W. R. Thiel, *Angew. Chem., Int. Ed.*, 2010, **49**, 3428–3459; (e) Y. Zhu, K. Loo, H. Ng, C. Li, L. P. Stubbs, C. F. Siong, M. Tan and S. C. Peng, *Adv. Synth. Catal.*, 2009, **351**, 2650–2656; (f) M. J. Jacinto, F. P. Silva, P. K. Kiyohara, R. Landers and L. M. Rossi, *ChemCatChem*, 2012, **4**, 698–703; (g) L. M. Rossi, M. A. S. Garcia and L. L. R. Vono, *J. Braz. Chem. Soc.*, 2012, **23**, 1959–1971.
- 20 G. Morral-Ruiz, P. Melgar-Lesmes, M. L. Garcia, C. Solans and M. J. Garcia-Celma, *Polymer*, 2012, **53**, 6072–6080.
- 21 (a) J. Kim, J. E. Lee, J. Lee, Y. Jang, S.-W. Kim, K. An, J. H. Yu and T. Hyeon, *Angew. Chem., Int. Ed.*, 2006, **45**, 4789–4793; (b) H. Xu, L. Cui, N. Tong and H. Gu, *J. Am. Chem. Soc.*, 2006, **128**, 15582–15583.
- 22 (a) M. Feyen, C. Weidenthaler, F. Schuth and A.-H. Lu, *Chem. Mater.*, 2010, **22**, 2955–2961; (b) L. P. Ramirez and K. Landfester, *Macromol. Chem. Phys.*, 2003, **204**, 22–31; (c) K. Landfester and L. P. Ramirez, *J. Phys.: Condens. Matter*, 2003, **15**, S1345–S1361.
- 23 P. A. Dresco, V. S. Zaitsev, R. J. Gambino and B. Chu, *Langmuir*, 1999, **15**, 1945–1951.
- 24 B. Zhang, J. M. Xing and H. Z. Liu, *Adsorption*, 2008, **14**, 65–72.
- 25 Y. Deng, L. Wang, W. Yang, S. Fu and A. Elaissari, *J. Magn. Magn. Mater.*, 2003, **257**, 69–78.
- 26 E. Weiss, B. Dutta, Y. Schnell and R. Abu-Reziq, *J. Mater. Chem. A*, 2014, **2**, 3971–3977.
- 27 (a) S. F. Chin, S. C. Pang and C. H. Tan, *J. Mater. Environ. Sci.*, 2011, **2**, 299–302; (b) D. W. Matson, J. C. Linehan, J. G. Darab and M. F. Buehler, *Energy Fuels*, 1994, **8**, 10–18; (c) S. Sun and H. Zeng, *J. Am. Chem. Soc.*, 2002, **124**, 8204–8205.
- 28 (a) J. Wang, J. Sun, Q. Sun and Q. Chen, *Mater. Res. Bull.*, 2003, **38**, 1113–1118; (b) Y.-h. Zheng, Y. Cheng, F. Bao and Y.-s. Wang, *Mater. Res. Bull.*, 2006, **41**, 525–529.
- 29 J. A. Lopez Perez, M. A. Lopez Quintela, J. Mira, J. Rivas and S. W. Charles, *J. Phys. Chem. B*, 1997, **101**, 8045–8047.
- 30 R. Massart, *IEEE Trans. Magn.*, 1981, **MAG-17**, 1247–1248.
- 31 R. Abu-Reziq, D. Wang, M. Post and H. Alper, *Chem. Mater.*, 2008, **20**, 2544–2550.
- 32 (a) J. Tsuji, *Palladium Reagents and Catalysts: Innovations in Organic Synthesis*, Wiley, 1995; (b) P. M. Henry, in *Advances in Organometallic Chemistry*, ed. F. G. A. Stone and W. Robert, Academic Press, 1975, vol. 13, pp. 363–452.
- 33 J. K. Cho, R. Najman, T. W. Dean, O. Ichihara, C. Muller and M. Bradley, *J. Am. Chem. Soc.*, 2006, **128**, 6276–6277.
- 34 C. Ramarao, S. V. Ley, S. C. Smith, I. M. Shirley and N. DeAlmeida, *Chem. Commun.*, 2002, 1132–1133.
- 35 S. V. Ley, C. Mitchell, D. Pears, C. Ramarao, J.-Q. Yu and W. Zhou, *Org. Lett.*, 2003, **5**, 4665–4668.
- 36 C. D. Wagner, W. M. Riggs, L. E. Davis, J. F. Moulder and B. E. Muilenberg, *Handbook of X-ray Photoelectron Spectroscopy*, Perkin-Elmer, Physical Electronics Division, Eden Prairie, 1979.
- 37 *Catalytic Hydrogenation*, ed. L. Červený, Elsevier Science Publishers B. V., Amsterdam, 1986.
- 38 (a) J. Kijenski, P. Winiarek, T. Paryczak, A. Lewicki and A. Mikolajska, *Appl. Catal., A*, 2002, **233**, 171–182; (b) H.-Y. Lee and M. An, *Tetrahedron Lett.*, 2003, **44**, 2775–2778; (c) E. Keinan and N. Greenspoon, *J. Am. Chem. Soc.*, 1986, **108**, 7314–7325; (d) P. Claus, *Top. Catal.*, 1998, **5**, 51–62.
- 39 (a) P. Gallezot and D. Richard, *Catal. Rev.: Sci. Eng.*, 1998, **40**, 81–126; (b) C. Mohr, H. Hofmeister, M. Lucas and P. Claus, *Chem. Eng. Technol.*, 2000, **23**, 324–328; (c) L. A. Saudan, *Acc. Chem. Res.*, 2007, **40**, 1309–1319.
- 40 (a) G. Wienhoefer, F. A. Westerhaus, K. Junge, R. Ludwig and M. Beller, *Chem.–Eur. J.*, 2013, **19**, 7701–7707; (b) S. Ganji, S. Mutyala, C. K. P. Neeli, K. S. R. Rao and D. R. Burri, *RSC Adv.*, 2013, **3**, 11533–11538; (c) K. H. Lim, A. B. Mohammad, I. V. Yudanov, K. M. Neyman, M. Bron, P. Claus and N. Rosch, *J. Phys. Chem. C*, 2009, **113**, 13231–13240; (d) Y. Yabe, Y. Sawama, Y. Monguchi and H. Sajiki, *Catal. Sci. Technol.*, 2014, **4**, 260–271; (e) H. G. Manyar, B. Yang, H. Daly, H. Moor, S. McMonagle, Y. Tao, G. D. Yadav, A. Goguet, P. Hu and C. Hardacre, *ChemCatChem*, 2013, **5**, 506–512; (f) Y. Himeda, N. Onozawa-Komatsuzaki, S. Miyazawa, H. Sugihara, T. Hirose and K. Kasuga, *Chem.–Eur. J.*, 2008, **14**, 11076–11081.